Springer

Journal of
Mechanical
Science and
Technology

Journal of Mechanical Science and Technology 22 (2008) 411~419

www.springerlink.com/content/1738-494x

Effects of fiber aspect ratio evaluated by elastic analysis in discontinuous composites

Hong Gun Kim*

Department of Mechanical and Automotive Engineering, Jeonju University, Jeonju, 560-759, Korea

(Manuscript Received January 1, 2007; Revised December 21, 2007; Accepted December 12, 2007)

Abstract

An elastic stress analysis to investigate the effects of fiber aspect ratio in short fiber reinforced discontinuous composite materials has been done for different fiber volume fractions. In order to examine the elastic internal behavior, an evaluation of the load bearing capacity of discontinuous reinforcements is needed in advance. Accordingly, analytical derivation of composite mechanics has been carried out to predict fiber stresses and fiber/matrix interfacial shear stresses in discontinuous composites. The model is based on the theoretical development of conventional shear lag theory developed by Cox. However, the major shortcoming of the Cox model is due to the calculation without normal stress transfer from the end of fibers. In order to overcome the shortcoming, both of the normal and shear stress transfer mechanisms between the fiber and the matrix are accounted for with the stress concentration effects as well as material and geometrical properties. Results of predicted stresses concerning the various fiber aspect ratios are described by using the present model that is the closed form solution and compared with the Cox model and Taya model. It is found that the effect of fiber aspect ratio is significant to composite strengthening through load transfer from the matrix to the fiber, whereas the effect of fiber volume fraction is not so sensitive, relatively. It is also found that the present model has the capability to correctly predict the values of fiber stresses and fiber/matrix interfacial shear stresses.

Keywords: Elastic stress analysis; Discontinuous composite; Fiber stress; Interfacial shear stress; Aspect ratio; Fiber volume fraction

1. Introduction

Composite materials are one of the strongest candidates as a structural material for many automobile, aerospace and other applications [1]. Recently, short fiber-reinforced composite materials have been extensively investigated because they are more economical and impact resistant [2]. One of the earliest attempts to explain the reinforcing effect of fibers was described by [3], and is now referred to as the shear lag theory, which considers long straight discontinuous fibers completely embedded in a continuous matrix [3, 4].

However, it does not provide sufficiently accurate strengthening predictions in elastic regime when the fiber aspect ratio is small [5, 6]. The predicted modulus obtained by conventional shear lag model is also substantially smaller than the experimentally observed values in the short fiber composites. As the fiber aspect ratio becomes small, the conventional shear lag model is not possible to provide accurate strengthening predictions in elastic regime. In fact, the conventional shear lag model underestimates the strength due to the neglect of stress transfer across the fiber ends, which exists in the matrix regions between fiber ends [7-9].

Nardone and Prewo [5] attempted to modify the conventional shear lag model by the concept to take into account the tensile transfer of load from the matrix to the discontinuous reinforcement. Their modified shear lag model is well fitted with the experimental data for prediction of yield strength of discontinuous composites though it is limited to predict the fiber

*Corresponding author. Tel.: +82 63 220 2613, Fax.: +82 63 220 2056
E-mail address: hkim@jj.ac.kr
DOI 10.1007/s12206-007-1208-1

stress with constant value after matrix yielding, which does not have the capability to calculate an estimation of elastic behavior. There have been more attempts such as Taya and Arsenault [10] considering reinforced fiber end stress as the average stress of matrix, though it has the limitation of no stress intensification between fibers.

To analyze the internal quantities such as fiber stresses and fiber/matrix interfacial shear stresses accurately, some major strengthening factors should be taken into account. Especially, the stress concentration phenomenon has to be incorporated for the accurate prediction of reinforcement effects. Accordingly, to exploit the more accurate and relatively simple model when the fiber and matrix are both in elastic regime, the present model that accounts for fiber end stresses in a simplified yet realistic manner is derived and the fiber aspect ratio effects are investigated in this paper.

Thus far, the stress transfer mechanism is considered for discontinuous composites with cylindrical fibers in the fiber-elastic and matrix-elastic regime. It is explained that the stress concentration effect near fiber ends enhances the load bearing capacity of the fiber and results in composite strengthening substantially. The quantitative study of the fiber aspect ratio effects is mainly focused on the composite strengthening. The present model gives a reasonable closed form solution and has the capability to correctly predict the values of fiber stresses and fiber/matrix interfacial shear stresses in the elastic regime.

2. Model development

2.1 Conventional shear lag concept

For a thorough understanding of the behavior of discontinuous composites, it is necessary to first understand the mechanism of stress transfer. A micromechanical model is described in Fig. 1. The short fibers are considered to be uniaxially aligned with the stress applied in the axial direction of the fibers. The axial direction is the *z*-axis and fiber diameter is *d*. The composite unit cell showing the short fiber embedded in a continuous matrix is shown in Fig. 1 and Fig. 2(a). The outer surface of the unit cell can be considered having a hexagonal contour. However, the exact shape is not critical in this model. Thus, the unit cell is treated as an equivalent cylinder and it can consequently be selected as RVE (Representative Volume Element) as shown in Fig. 1 and Fig. 2(a). The short fibers are considered to be uniaxially aligned with the stress applied in the axial direction of the fibers. Further, no plastic yielding is allowed, that is, both matrix and fiber deform in a purely elastic manner. The axial direction is the *z*-axis and displacement is *w*.

In Fig. 1(b), the axial displacement can have two folds like the upper and lower bounds in association with fiber direction and in-between fiber direction. However, the upper bounds of axial displacement are implemented in this study since there is the more reasonable rationale choosing a boundary with neighboring RVE. Accordingly, the displacement of fiber and RVE surface in the *z*-direction is w_f and w_R as shown in Fig. 1(b), respectively. The diameter of fiber and RVE is r_f and R.. Likewise, the shear stress of fiber surface and arbitrary surrounding matrix in the *z*-direction is τ_e and τ, respectively. The proposed composite unit cell showing the unstrained and strained RVE in a discontinuous composite is shown in Fig. 2(a) and (b). Here, the fiber radius is fixed as unit length, i.e., r_f=1, so that the aspect ratio, *s*, has the same length of the normalized fiber distance. In Fig. 2(d), SCF means stress concentration factor, which is accounted for by the unit value [2] and the value as a function of modulus ratio to be described by α_k in a later section.

In Fig. 1, shear forces at arbitrary distance with r and those at the fiber surface r_f in the composite element are

$$2\pi r\tau\, dz = 2\pi r_f \tau_e dz \quad \text{or} \quad \tau = r_f\tau_e / r,\ \ r_f \le r \le R \tag{1}$$

Shear deformation ratio dw/dr over the shear stress becomes the shear elastic modulus of the matrix G_m:

$$\frac{dw}{dr} = \frac{\tau}{G_m} = \frac{\tau_e r_f}{G_m r} \tag{2}$$

Integrating Eq. (2),

$$\int_{w_f}^{w_R} dw = \frac{\tau_e r_f}{G_m}\int_{r_f}^{R}\frac{dr}{r} \tag{3}$$

It results in Eq. (4).

$$w_R - w_f = \frac{\tau_e r_f}{G_m}\ln(R/r_f) \tag{4}$$

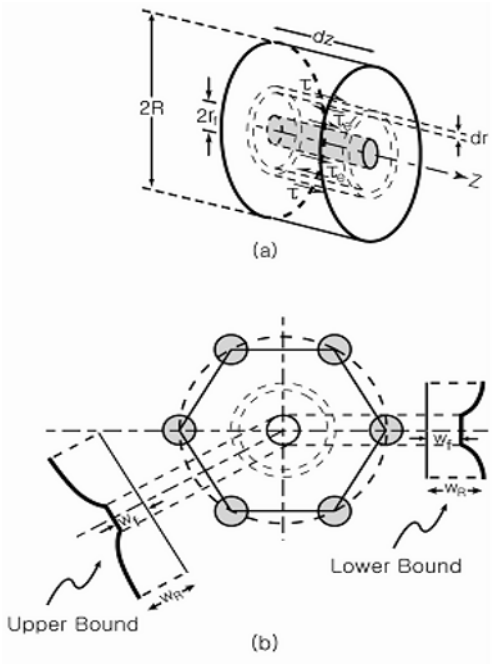

Fig. 1. Schematic of short length of fiber and surrounding matrix. (a) Small volume for equilibrium, (b) Fiber with nearest neighbors and associated displacements along the fiber axis.

Hence, $(w_R - w_f)$ means the displacement and shear stress of the RVE surface in the *z*-direction.

On the other hand, R/r_f depends on the reinforcement arrangement. The area of square in case of square arrangement is R^2 and the fiber volume fraction can be $V_f = \frac{\pi r_f^2}{R^2}$. Thus, the relationship of fiber arrangement becomes as below:

$$\ln(\frac{R}{r_f}) = \frac{1}{2}\ln(\frac{\pi}{V_f}) \tag{5}$$

In the same fashion, the hexagonal arrangement of fibers shown in Fig. 1(b) has the following relation:

$$\ln(\frac{R}{r_f}) = \frac{1}{2}\ln(\frac{2\pi}{\sqrt{3}V_f}) \tag{6}$$

However, the difference of the above two cases is not very large and Eq. (7) can be derived.

$$\ln(\frac{R}{r_f}) = \frac{1}{2}\ln(\frac{P_f}{V_f}) \tag{7}$$

Hence, packing factor $P_f = \frac{2\pi}{\sqrt{3}}$. Substituting Eq. (7) into Eq. (4) gives Eq. (8).

$$\tau_e = \frac{E_m(W_R - W_f)}{(1+v_m)r_f \ln(P_f/V_f)} \tag{8}$$

where $G_m = \frac{E_m}{2(1+v_m)}$

Hence, the fiber axial stress and the fiber/matrix interfacial shear stress have a relationship as in Eq. (9), which is the equilibrium equation:

$$\frac{d\sigma_f}{dz} = -\frac{2\tau_e}{r_f} \tag{9}$$

Where σ_f is the fiber axial stress. Substituting Eq. (8) into Eq. (9),

$$\frac{d\sigma_f}{dz} = -\frac{2E_m(w_R - w_f)}{(1+v_m)r_f^2 \ln(\frac{P_f}{V_f})} \tag{10}$$

On the other hand, implementing the relationship between fiber displacement w_f and fiber axial strain ε_f,

$$\varepsilon_f = \frac{dw_f}{dz} \tag{11}$$

Therefore

$$\frac{dw_f}{dz} = \frac{\sigma_f}{E_f} \tag{12}$$

Hence, assuming $\frac{dw_R}{dz} = \varepsilon_c$ when $r = R$, Eq. (13) can be achieved by differentiated expression of Eq. (11).

$$\frac{d^2\sigma_f}{dz^2} = -\frac{2E_m(\varepsilon_c - \sigma_f/E_f)}{(1+v_m)r_f^2 \ln(P_f/V_f)} \tag{13}$$

Here, E_m, E_f and v_m are Young's moduli of the matrix and the fiber and Poisson's ratio of the matrix, respectively. Hence the governing is obtained as Eq. (14).

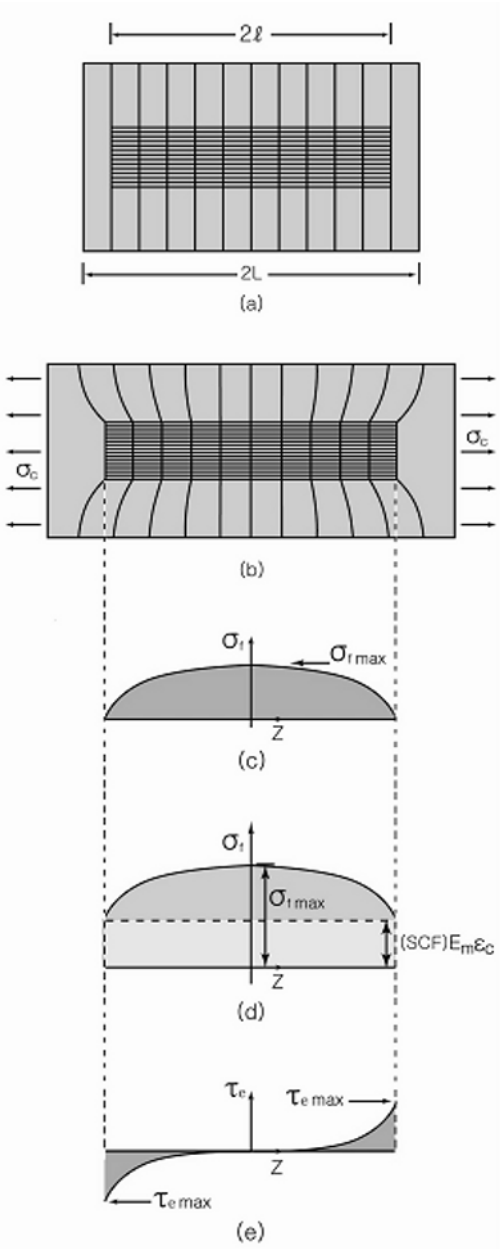

Fig. 2. Single fiber composite element of the elastic fiber and matrix. (a) Unstrained RVE, (b) Strained RVE, (c) The fiber axial stress for Cox model, (d) The fiber axial stress for Kim model, (e) The fiber/matrix interfacial shear stress for elastic stress transfer.

$$\frac{d^2\sigma_f}{dz^2} = -\frac{n^2}{r_f^2}(\sigma_f - E_f\varepsilon_c) \tag{14}$$

Where n is the dimensionless parameter associated with Eq. (15).

$$n^2 = \frac{2E_m}{E_f(1+\nu_m)\ln(P_f/V_f)} \tag{15}$$

Then, the above equation admits a solution as shown below. Here, ε_c is the far-field composite strain. Eq. (14) has the solution as

$$\sigma_f = E_f\varepsilon_c + A\sinh(\frac{nz}{r_f}) + B\cosh(\frac{nz}{r_f}) \tag{16}$$

Here A and B are unknown constants which need to be determined from the following boundary conditions by assuming that no stress is transferred across the fiber ends as depicted in Fig. 2(c).

$$r_f = 0 \quad \text{at} \quad z = \pm l \tag{17}$$

Thus,

$$A = 0\,, \quad B = -\frac{E_f\varepsilon_c}{\cosh(ns)} \tag{18}$$

where $s(=l/r_f)$ is fiber aspect ratio. Therefore, the fiber axial stress and the fiber/matrix interfacial shear stress are obtained as follows:

$$\sigma_f^{Cox} = E_f\varepsilon_c\left\{1 - \frac{\cosh(nz/r_f)}{\cosh(ns)}\right\} \tag{19}$$

$$\tau_e^{Cox} = \left(\frac{nE_f\varepsilon_c}{2r_f}\right)\frac{\sinh(nz/r_f)}{\cosh(ns)} \tag{20}$$

2.2 Formulation of the New Model

In short fiber composites, loads are not directly applied on the fibers but are applied to the matrix and transferred to the fibers through the fiber ends as well as through the cylindrical surface of the fiber. When the length of a fiber is much greater than the length over which the transfer of stress takes place, the end effects can be neglected. The end effects significantly influence the behavior and reinforcing effects in a short fiber-reinforced discontinuous composite.

Taya and Arsenault [2] reported the fiber axial stress by taking fiber end stress into account without stress concentration effect. Accordingly, fiber end stress is imposed by the far field average matrix stress as interfacial condition in Eq. (17), which is expressed as Eq. (21):

$$\sigma_f = \sigma_i = E_m \varepsilon_c \quad \text{for} \quad z = \pm l \tag{21}$$

where σ_i is interfacial fiber axial stress at the fiber ends. Therefore, their equation can be given by Eq. (22).

$$\sigma_f^{Taya} = E_f \varepsilon_c \left\{ 1 + \left(\frac{E_m}{E_f} - 1 \right) \frac{\cosh(nz/r_f)}{\cosh(ns)} \right\} \tag{22}$$

For the Taya model, the formulation of the fiber/matrix interfacial shear stress at the fiber surface has not been specified in detail. But it can be derived easily here by using the differentiation procedure and the result becomes as below:

$$\tau_e^{Taya} = \frac{nE_f \varepsilon_c}{2r_f} \left(1 - \frac{E_m}{E_f} \right) \frac{\sinh(nz/r_f)}{\cosh(ns)} \tag{23}$$

However, it is found that their prediction is fairly underestimated because of the neglected stress intensification at fiber ends [7, 9, 11]. Hence, fiber end stress including stress concentration effect should be implemented as a boundary condition in Eq. (21). Thus Eq. (24) will be the more accurate fiber/matrix axial interfacial condition:

$$\sigma_i = \alpha_k E_m \varepsilon_c \quad \text{for} \quad z = \pm l \tag{24}$$

Where α_k is the stress concentration factor (SCF in Fig. 2(d)) between the fiber end and the matrix, which can be evaluated as a square root function of modulus ratio [12]. The physical meaning of α_k can be expressed as the maximum axial stress ratio out of the average stress in the matrix. Thus, α_k can be expressed in Eq. (25) as (SCF) depicted in Fig. 2(d).

$$\alpha_k = \sqrt{\frac{E_f}{E_m}} \tag{25}$$

Substituting Eq. (25) into Eq. (24), the interfacial fiber axial stress at fiber ends σ_i is obtained as below.

$$\sigma_i = \sqrt{E_f E_m}\, \varepsilon_c \tag{26}$$

As formulated by now, the fiber axial stress and the fiber/matrix interfacial shear stress are derived as follows:

$$\sigma_f^{Kim} = E_f \varepsilon_c \left\{ 1 + \left(\sqrt{\frac{E_m}{E_f}} - 1 \right) \frac{\cosh(nz/r_f)}{\cosh(ns)} \right\} \tag{27}$$

$$\tau_e^{Kim} = \frac{nE_f \varepsilon_c}{2r_f} \left(1 - \sqrt{\frac{E_m}{E_f}} \right) \frac{\sinh(nz/r_f)}{\cosh(ns)} \tag{28}$$

On the other hand, there are several other models for the prediction. The rule of mixture model (ROM) shows an overestimated prediction for discontinuous composites since it is exactly the case of continuous composites. However, the fiber axial stresses predicted by the Cox and Taya model are clearly underestimated, though the Taya model is a little higher than the Cox model.

3. Results and discussion

The results of the present study (Kim model) are focused on fiber aspect ratio effects and summarized with the Cox and Taya model for comparison. For numerical calculation, typical elastic moduli of materials are chosen as E_f=480GPa for the fiber and E_m=70GPa for the matrix. The fiber volume fraction V_f is imposed with two cases of V_f=20% and V_f=40%. The far field strain or applied composite strain is imposed by 0.1% in all following analyses because of securing enough small strain of elastic behavior.

In Figs. 3 to 6, the prediction of internal quantities of stress field in a single fiber model (RVE) is carried out by varying fiber aspect ratios of 4, 8, 16 and 32, respectively. Fig. 3 shows fiber axial stresses for different fiber aspect ratios in the case of V_f=20%. The fiber axial stress is influenced significantly by the fiber aspect ratio, whereas it is slightly influenced by the fiber volume fraction as can be seen in Fig. 3. Effects of the fiber aspect ratio are also quantitatively calculated with more accurate prediction by the present model. In the previous study [12], fiber axial stresses calculated by the present model give the most accurate agreement with FEA results.

Fig. 3(a) shows a great discrepancy between the results of the Cox, Taya and present (Kim) models, which indicates that the difference is caused by either taking fiber end stresses or stress concentration effects into account in the conventional shear model. It is obvious that the results of the Cox model are substantially underestimated compared to other two models. The Taya model is also underestimated due

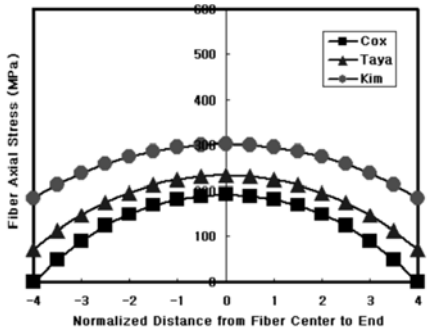

(a) s=4, V_f=20%

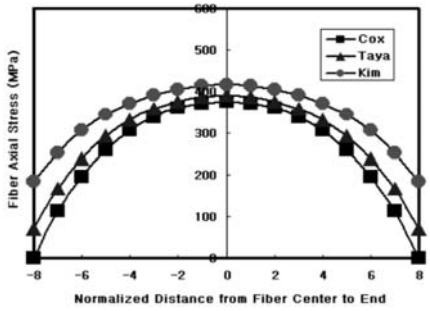

(b) s=8, V_f=20%

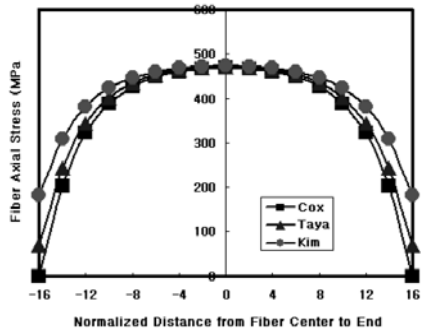

(c) s=16, V_f=20%

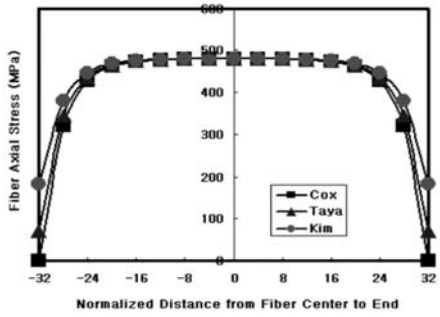

(d) s=32, V_f=20%

Fig. 3. Fiber axial stresses according to the change of fiber aspect ratio in case of V_f=20%.

to the neglecting of stress concentration effects, though it is an improved model from the Cox model. In Fig. 3(b) to (d), however, it is shown that the discrepancy of fiber axial stresses becomes smaller as the fiber aspect ratio becomes larger.

Fig. 4 shows fiber axial stresses for a different fiber aspect ratio in the case of V_f=40%. Fig. 4(a) also shows a great discrepancy between the results of the Cox, Taya and present (Kim) models. In Fig. 4(b) to (d), however, it is shown that the discrepancy of fiber axial stresses becomes smaller as the fiber aspect ratio becomes larger as in the case of V_f=20%.

The fiber volume fraction effects are compared in Figs. 3 and 4. The fiber axial stresses show a slight increase as fiber volume fraction becomes larger. It is shown that the effect of fiber volume fraction is fairly restricted to the short fiber reinforcement and little discrepancy is found for the large fiber aspect ratio value. Furthermore, the fiber axial stresses are nearly saturated from over s=16 independent of fiber volume fraction. In all cases, however, all three models converge to the same value when the fiber aspect ratio becomes infinity as it should.

Fig. 5 shows fiber/matrix interfacial shear stresses for different fiber aspect ratios in the case of V_f=20%. The fiber/matrix interfacial shear stress is also influenced substantially by the fiber aspect ratio, whereas it is slightly influenced by the fiber volume fraction as in the case of the fiber axial stress. Effects of the fiber aspect ratio are quantitatively compared for all three models in Fig. 5. Fig. 5(a) shows a discrepancy between the results of the Cox, Taya and present models as varying the fiber aspect ratio, which indicates that the amount of difference is relatively less sensitive than the case of fiber axial stresses. It is also caused by either taking fiber end stresses or stress concentration effects into account in the conventional shear model. It is shown that the results of the Cox model are overestimated compared to other two models. In Fig. 5(b) to (d), however, the discrepancy of fiber/matrix interfacial shear stresses varies a little as the fiber aspect ratio becomes larger. It is found that the fiber/matrix interfacial shear stress is nearly saturated at the center region of the fiber in Fig. 5(d).

Fig. 6 shows fiber/matrix interfacial shear stresses for the different fiber aspect ratio in case of V_f=40%. Fig. 6(a) also shows a discrepancy between the results of the Cox, Taya and present (Kim) models. In Fig. 6(b) to (d), however, the discrepancy of fiber/matrix interfacial shear stresses varies a little as the fiber

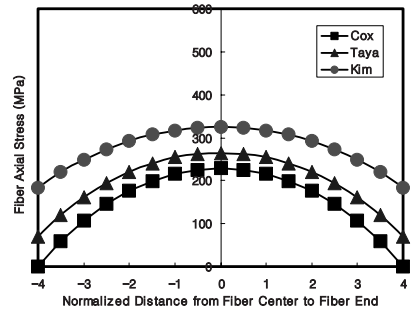

(a) s=4, V_f=40%

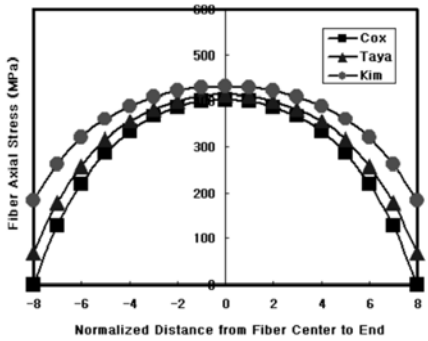

(b) s=8, V_f=40%

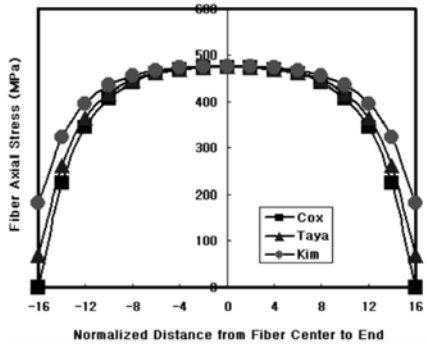

(c) s=16, V_f=40%

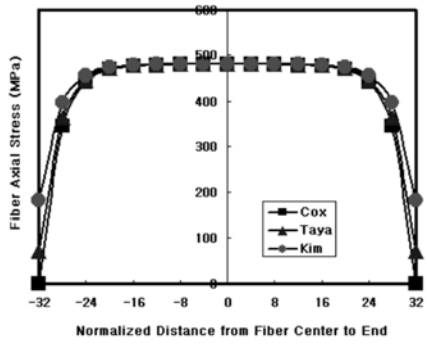

(d) s=32, V_f=40%

Fig. 4. Fiber axial stresses according to the change of fiber aspect ratio in case of V_f=40%.

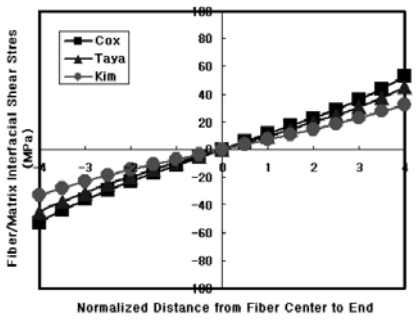

(a) s=4, V_f=20%

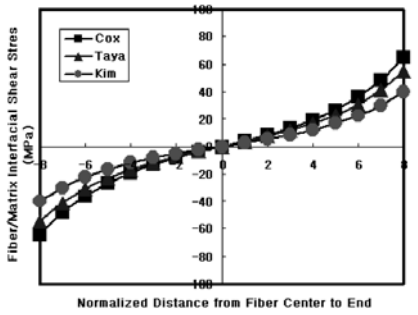

(b) s=8, V_f=20%

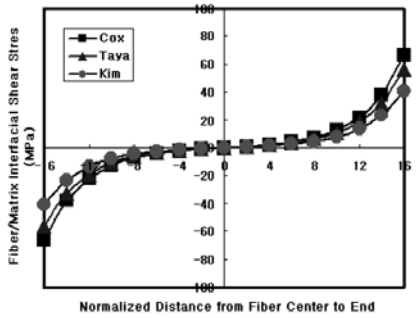

(c) s=16, V_f=20%

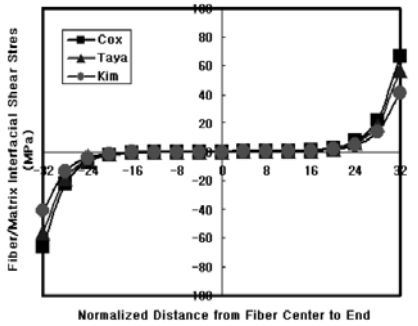

(d) s=32, V_f=20%

Fig. 5. Fiber/matrix interfacial shear stresses according to the change of fiber aspect ratio in case of V_f=20%.

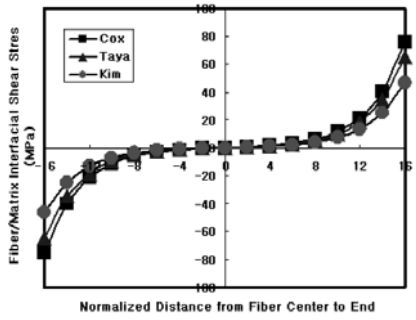

(a) s=4, V_f=40%

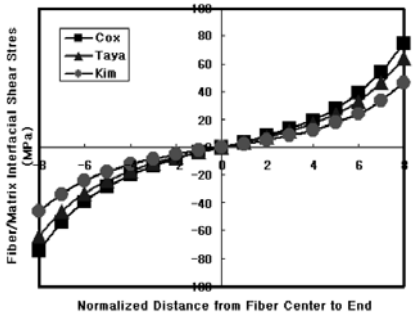

(b) s=8, V_f=40%

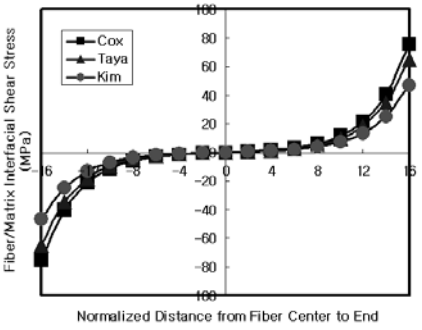

(c) s=16, V_f=40%

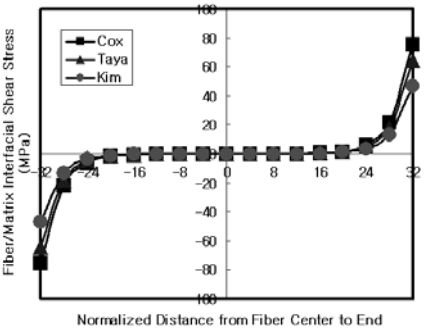

(d) s=32, V_f=40%

Fig. 6. Fiber/matrix interfacial shear stresses according to the change of fiber aspect ratio in case of V_f=40%.

aspect ratio becomes larger like the results of V_f=20%. Also, the fiber/matrix interfacial shear stress is not so sensitive to the fiber volume fraction. At the center region of the fiber in Fig. 6(d), the fiber/matrix interfacial shear stress is nearly saturated.

4. Conclusions

The effects of fiber aspect ratio in short fiber reinforced discontinuous composite materials were studied for two different fiber volume fractions (20% and 40%). It was found that fiber axial stresses are substantially influenced by fiber aspect ratios and are more sensitive when the fiber aspect ratio becomes smaller. However, they are fairly sensitive below s=16 of fiber aspect ratio and show nearly saturated value above s=16. It was also found that the fiber axial stresses of the Cox, Taya and present (Kim) models converge to the same value as they should do when the fiber aspect ratio becomes infinity. Fiber axial stresses increase as the fiber volume fraction increases, though not as sensitive as compared to the fiber aspect ratio effects. The effect of fiber volume fraction is fairly restricted to the very short fiber reinforcement, while little discrepancy is found for the large fiber aspect ratio.

Fiber/matrix interfacial shear stresses between the Cox and Taya model do not show a significant difference, though the present model is lower than those of the models in all cases. On the other hand, fiber aspect ratios affecting the fiber/matrix interfacial shear stresses are not so sensitive compared to fiber axial stresses. The fiber axial stress and fiber/matrix interfacial shear stress is nearly saturated at the center region of the fiber when the fiber aspect ratio is increased. Also, the stress saturation value of the fiber aspect ratio is about s=16.

References

[1] B. D. Agarwal, J. M. Lifsitz and L. J. Broutman, Elastic plastic finite element analysis of short fiber composites, Fib. Sci. Tech. 7 (1974) 45-62.

[2] M. Taya and R. J. Arsenault, Metal Matrix Composites-Thermomechanical Behavior, Pergamon Press, USA, (1989).

[3] H. L. Cox, The elasticity and strength of paper and other fibrous materials, *Brit. J. Appl. Phy.* 3 (1952) 72- 79.

[4] B. D. Agarwal and L. J. Broutman, Analysis and Performance of Fiber Composites, John Wiley and

Sons, New York, USA, (1980).

[5] V. C. Nardone and K. M. Prewo, On the strength of discontinuous silicon carbide reinforced aluminum composites, *Scr. Meta.* 20 (1986) 43-48.

[6] B. Ji and T. Wang, Constitutive behaviors of discontinuous reinforced composites," *Key Eng. Mat.* 177-180 (2000) 297-302.

[7] T. W. Clyne, A simple development of the shear lag theory appropriate for composites with a relatively small modulus mismatch, *Mat. Sci. Eng.* A122 (1989) 183-190.

[8] H. G. Kim, Analytical study on the elastic-plastic transition in short fiber reinforced composites, *KSME Int. J.* 12 (2) (1998) 257-266.

[9] M. J. Starink and S. Syngellakis, Shear lag models for discontinuous composites: fibre end stresses and weak interface layers, *Mat. Sci. Eng.* A270 (1999) 270-277.

[10] M. Taya and R. J. Arsenault, A comparison between a shear lag type model and an Eshelby type model in predicting the mechanical properties of short fiber composite, *Scr. Meta.* 21 (1987) 349-354.

[11] Z. Jiang, An analytical study of the influence of thermal residual stresses on the elastic and yield behaviors of short fiber-reinforced metal matrix composites, *Mat. Sci. Eng.* A248 (1998) 256-275.

[12] H. G. Kim and H. G. Noh, Effects of elastic modulus ratio on internal stresses in short fiber composites, *J. Kor. Soc. Mach. Tool Eng.* 13 (4) (2004) 73-78.